Heteroatom Chemistry
Volume 18, Number 5, 2007

Conformationally Induced Electrostatic Stabilization (CIES) of Persulfoxides. A Comparison to Homologous Sulfoxides

Edward L. Clennan and Sean E. Hightower

Department of Chemistry, University of Wyoming, Laramie, WY 82071

Received 5 October 2006; revised 16 October 2006

ABSTRACT: *Computational and experimental evidence that participation of a remote heteroatom occurs during the formation and decomposition of persulfoxides is presented. The experimental ramifications of remote participation includes a dramatic increase in the rate of reaction with singlet oxygen and a decrease in the conformationally dependent ability of sulfides to physically deactivate singlet oxygen. The ability of different heteroatoms to participate is evaluated with a natural bond orbital analysis, and a comparison of the extent of participation in persulfoxides and their homologous sulfoxides is presented.* © 2007 Wiley Periodicals, Inc. Heteroatom Chem 18:591–599, 2007; Published online in Wiley InterScience (www.interscience.wiley.com). DOI 10.1002/hc.20343

INTRODUCTION

The use of molecular oxygen as a terminal oxidant is both economically and environmentally attractive. Unfortunately, the triplet ground state coupled with the small size of dioxygen has made molecular oxygenations notoriously difficult to control. On the other hand, there are two low-lying metastable singlet excited states ($^1\Delta_g$ and $^1\Sigma_g^+$) of dioxygen [1]. The dioxygen $^1\Delta_g$ state lies approximately 22.5 kcal mol^{-1}, and the $^1\Sigma_g^+$ state approximately 37 kcal mol^{-1}, above the paramagnetic triplet ($^3\Sigma_g^-$) ground state. The $^1\Delta_g$ state, but not the $^1\Sigma_g^+$ state, has a sufficient lifetime to undergo bimolecular reactions with organic substrates and is sufficiently influenced by steric, hydrogen bonding, and stereoelectronic effects to render it synthetically useful [2–4]. In addition to its synthetic utility, singlet oxygen ($^1\Delta_g$) has also been used as a cytotoxic agent to destroy cancerous tumors in a process called photodynamic therapy [5–7]. Consequently, the mechanistic details of its reactions with sulfur centers that are ubiquitous in biomolecules are of special interest.

The first example of the reaction of singlet oxygen ($^1\Delta_g$) with a sulfide was reported in 1962 by Schenck and Krauch [8]. The intricacies of the potential energy surface of this surprisingly complex reaction are now reasonably well understood and are depicted in Scheme 1 [9]. The mechanism involves two intermediates, a persulfoxide, **1**, and a hydroperoxy sulfonium ylide, **2**. The persulfoxide is only weakly bound, and its decomposition to triplet oxygen and the sulfide substrate is responsible for the very low quantum yields typically observed in these reactions [10].

The ability of an intramolecular nucleophile to add to the sulfonium sulfur of the persulfoxide intermediate, **1**, was demonstrated as early as 1977 with the elegant study of methonine photooxygenation [11]. However, until recently [12] no systematic study of the conformational features of the substrates, the influence of the identity of the remote nucleophile (heteroatom), or the influence of the heteroatom on the overall efficiency of the reaction had been undertaken. In this paper, we describe the

Correspondence to: Edward L. Clennan; e-mail: clennane@uwyo.edu.
Contract grant sponsor: National Science Foundation.
Contract grant number: CHE-0313657.

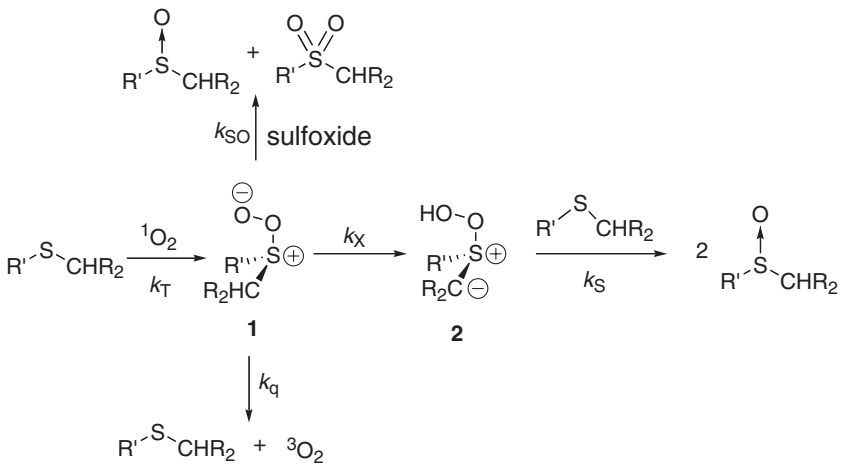

SCHEME 1

influence of a remote heteroatom on the photooxygenations of a series of five-heteroatom substituted cyclooctylsulfides, **3**, and a comparison of the interaction of the heteroatom in the persulfoxide intermediates, **3PS**, and in the homologous sulfoxides, **3SO**.

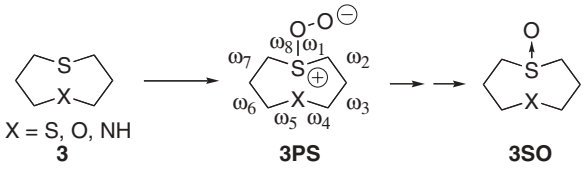

RESULTS AND DISCUSSION

Product Analysis

The reaction of singlet oxygen ($^1\Delta_g$) with 1,5-dithiacyclooctane, **3**(X = S) is mechanistically well behaved, conforming well to the generic mechanism depicted in Scheme 1. Photolysis of high concentrations (0.05–0.10 M) of **3**(X = S) and Rose Bengal (2×10^{-5} M) gives exclusively the sulfoxide, **3SO**(X = S), that reacts further, upon extended irradiation at −80°C, to give cis-bissulfoxide with a mass balance of 100% [13]. In contrast, at 20°C, a mixture of both cis- and trans-bissulfoxides was obtained with a significantly reduced mass balance (Scheme 2). The byproducts formed at room temperature appear to be the ring cleavage products as reported by Foote and coworkers [14].

Kinetic Studies

The total rate constant for removal of singlet oxygen from solution by sulfides, k_T, is given by Eq. (1). In this equation, k_r is the rate constant for chemical reaction and k_q is the rate constant for physical quenching of singlet oxygen by the sulfide.

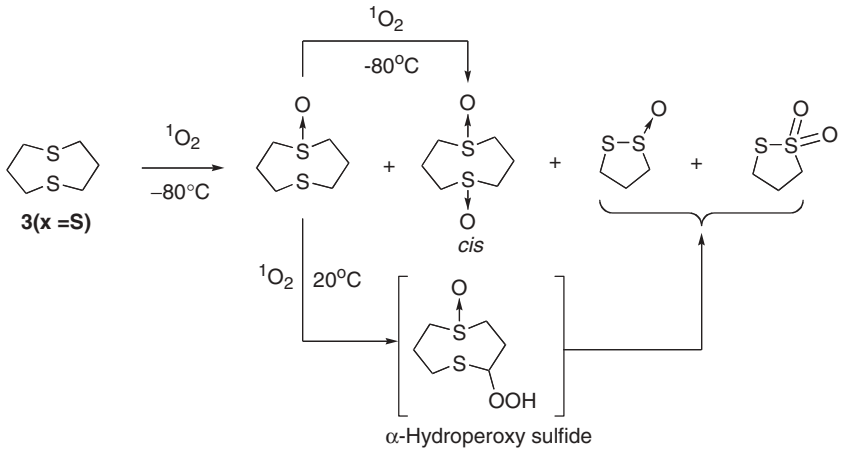

SCHEME 2

$$k_T = k_r + k_q \quad (1)$$

$$\frac{d[^1O_2]}{dt} = k_{obsd}[^1O_2] \quad (2)$$

$$k_{obsd} = k_T[3(X=S)] + k_d \quad (3)$$

The measured rate constants, k_{obsd}, for **3**(X = S) were measured by following the time-resolved decay of singlet oxygen at 1270 nm as a function of sulfide concentration and includes a contribution from the rate constant for the natural decay of singlet oxygen in acetone, k_d. (Eqs. (2) and (3)). The total rate constant ($k_T = 5.3 \times 10^7$ M^{-1} s^{-1}) was extracted by plotting k_{obsd} versus sulfide concentration according to Eq. (3). The chemical rate constant ($k_r = 3.73 \times 10^7$ M^{-1} s^{-1}) was measured by a competitive method [15] by measuring the rate of disappearance of **3**(X = S) relative to the rate of formation of the allylic hydroperoxide from reaction of 2,3-dimethyl-2-butene ($k_r = 2.7 \times 10^7$ M^{-1} s^{-1}) [16]. With k_T and k_r, in hand, k_q (1.57×10^7 M^{-1} s^{-1}) was determined by their difference (Eq. (1). These values indicate that 70% (i.e., $k_r/k_T = 0.70$) of the singlet oxygen is incorporated into product, and only 30% is physically deactivated during reaction of **3**(X = S).

Trapping Studies

Intermediates in sulfide photooxygenations are elusive as judged by the absence of any report of the direct spectroscopic observation of either a persulfoxide, **1**, or hydroperoxysulfonium ylide, **2**. Nevertheless, trapping experiments have provided compelling evidence for their presence on the reaction surface [17]. Diphenylsulfide, Ph_2S, and diphenylsulfoxide, Ph_2SO, are especially advantageous trapping agents since suitably substituted derivatives simultaneously report on the electronic character of the intermediate. Cophotooxidation of both of these trapping agents with **3**(X = S) resulted in their oxidations despite the fact that they are unreactive under the reaction conditions in the absence of the sulfide substrate. Plots of the product ratios during these trapping experiments as a function of the **3**(X = S) concentration are depicted in Fig. 1.

The observation of straight lines and the change in the slope of the lines when the ratio [**3SO**(X = S)]/[Ph_2SO] is plotted versus 1/[Ph_2S] (Fig. 1a) is consistent with competitive trapping of an intermediate by Ph_2S and **3**(X = S) as predicted in Scheme 1. Quantitative treatment of the mechanism (Scheme 1) using k_{PHS} as the rate constant for trapping of the hydroperoxysulfonium ylide by Ph_2S gives Eq. (4). The value of k_S/k_{PHS} of 20.8 extracted from this data indicates that **3**(X = S) is a much better trapping agent than Ph_2S. The insensitivity of the slope to the **3**(X = S) concentration in the sulfoxide trapping experiment (Fig. 1b) indicates that Ph_2SO and **3**(X = S) do not compete with each other for an intermediate, again consistent with the mechanism depicted in Scheme 1 and, quantitatively described by Eq. (5). The value of $k_X/k_{SO} = 1.16$ extracted from this data indicates that the efficiency of trapping and interconversion of the persulfoxide, **1**, to the hydroperoxy sulfonium ylide, **2**, is approximately the same in the reaction of **3**(X = S) with singlet oxygen.

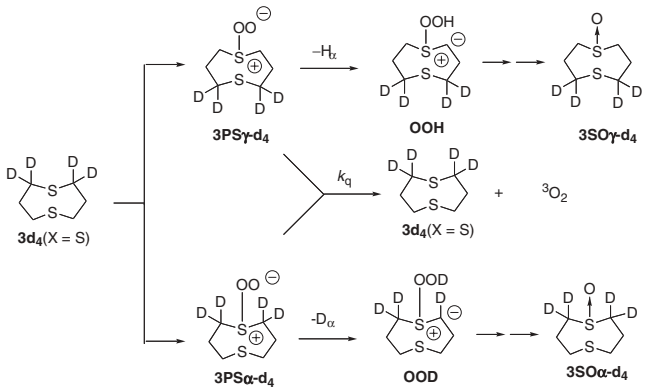

SCHEME 3

$$\frac{[3SO(X=S)]}{[Ph_2SO]} = 1 + \frac{2k_S[3(X=S)]}{k_{PHS}[Ph_2S]} \quad (4)$$

$$\frac{[3SO(X=S)]}{[Ph_2SO_2]} = 1 + \frac{2k_X}{k_{SO}[Ph_2SO]} \quad (5)$$

Isotope Effect Study

The formation of the hydroperoxy sulfonium ylide, **2**, during reaction of **3**(X = S) was established by examination of the d_4-isotopomer, **3d$_4$**(X = S), as shown in Scheme 3 [18]. The observation of a significant isotope effect ($k_H/k_D = 1.21 \pm 0.09$ = [**3SO**γ-**d$_4$**]/[**3SO**α-**d$_4$**]) is consistent with hydroperoxy sulfonium ylide formation. The preferred abstraction of hydrogen rather than deuterium allows formation of persulfoxide **OOH** to compete more effectively than formation of **OOD** with physical quenching, k_q, ultimately leading to a [**3SO**γ-**d$_4$**]/[**3SO**α-**d$_4$**] ratio greater than 1.

Computational Studies

The product studies, the trapping studies, and the kinetic isotope effect all suggest that **3**(X = S) conforms to the mechanism adopted (Scheme 1) by most simple dialkylsulfides. However, the kinetic

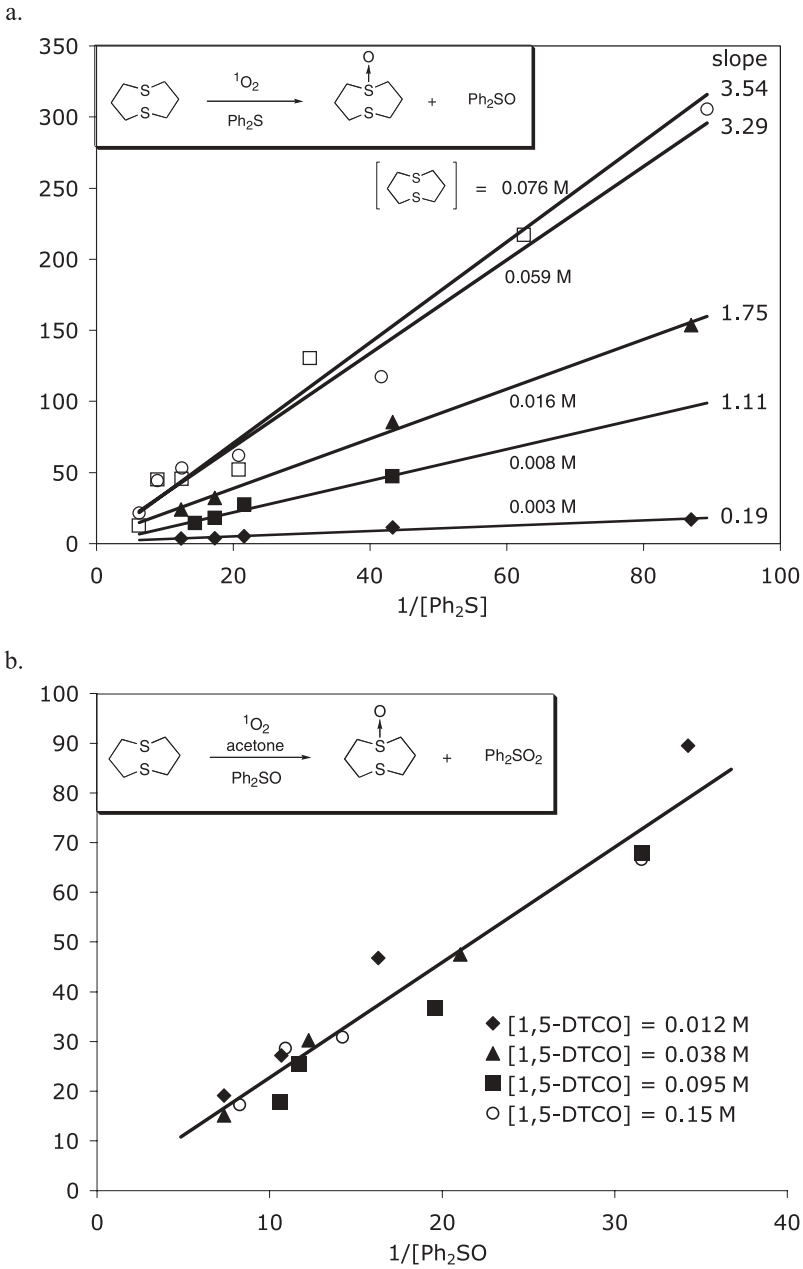

FIGURE 1 Product ratios, as a function of 1/[trapping agent] as a function of the concentration of **3**(X = S) for (a) diphenylsulfide and (b) diphenylsulfoxide trapping reactions.

data are unusual. In particular, the 70% efficiency (vide supra) for reaction of singlet oxygen with **3**(X = S) is unusually high. For example, diethylsulfide [17] and the simple six-membered ring thiane [12] react with less than 5% efficiency.

Since the efficiencies of singlet oxygen reactions are a direct result of partitioning of the persulfoxide intermediate (Scheme 1), we have computationally examined these key intermediates formed in the reaction of **3** and compared them to the homologous sulfoxides. Most of the computational studies were done at the MP2/6-31G(d) level, and the location of true minima was demonstrated by frequency calculations. Select persulfoxides and sulfoxides (Table 1) were also examined at the MP2/6-311+G(p,d) and the B3LYP/6-31G(d) level which demonstrated that the geometries at these levels of theory (MP2 and DFT) are fairly insensitive to the size of the basis set. The average deviation of the dihedral angles around the periphery of the persulfoxides, **3PS**(X = S), and

the sulfoxides, **3SO**(X = S), was greatest for **PS2** (±2.76°) and less that ±1.00° for all the other structures shown in Table 1.

The conformational potential energy surface for **3** is very complex; consequently, we have adapted the approach of Furukawa and coworkers [19] to ensure a reasonable sampling of conformational space and location of all important lower energy sulfoxides and persulfoxides. This method involves the following steps: (1) optimization of **3**(X = S) conformations generated by inserting the two sulfur atoms into the various locations in the well-established conformations of cyclooctane [20] followed by replacement of the sulfur with NH and O to generate **3**(X = NH, O), (2) addition of oxygen in various conformations to the sulfur and optimization in order to locate the persulfoxides, and (3) removal of the pendant oxygen on each of the persulfoxides and optimization to locate conformations of the sulfoxide. This protocol resulted in the identification of 18 persulfoxide conformations for **3** and 18 homologues sulfoxides. Only 4 of the 18 persulfoxide conformations located on the **3**(X = S) reaction surface have S—S intramolecular distances within the van der Waals radii (3.6 Å) [21] of two sulfur atoms. Remarkably, this list (Table 2) of four persulfoxides includes three of the most stable persulfoxide conformations. The homologous sulfoxides are also listed for comparison in Table 2. In every case, with the sole exception of **3PS5** and **3SO5**, the intramolecular S–S distance in the sulfoxides is greater than in the persulfoxides.

All of the persulfoxides adopt a geometry in which the O–O linkage is above the two α-carbons nearly bisecting the C—S^+—C bond (Fig. 2). The S—O and O—O bond lengths in the persulfoxides, **3PS** (X = S), were between 1.59–1.65 Å and 1.45–1.48Å, respectively. The S—O—O angles were 108° ± 4°, and the S^+ -pendant (remote) oxygen distance was 2.48 ± 0.06 Å well outside the distance (≤1.82 Å) [9] that could be construed to be an S—O bond in a three-membered ring thiadioxirane. The sulfoxide oxygens in the low-energy conformations depicted in Fig. 2 all adopt geometries that avoid destabilizing cross-ring interactions and have remarkably uniform S—O bond lengths of 1.52 ± 0.01 Å.

The core conformations of both the persulfoxides and the computationally derived sulfoxides are

TABLE 1 Persulfoxide, **3PS**(X = S), and Sulfoxide, **3SO**(X = S) Geometries (Ring Fragment Dihedral Angles) as a Function of Theory and Basis Set[a]

	Theory/Basis Set	ω_1	ω_2	ω_3	ω_4	ω_5	ω_6	ω_7	ω_8
PS1[b]	MP2/6-31G*	106.68	−71.28	66.11	−109.80	59.66	55.24	−68.29	−39.96
	MP2/6-311+G(d,p)	106.23	−71.11	66.38	−110.58	59.39	56.57	−70.09	−39.10
PS2	MP2/6-31G*	37.79	61.47	−40.16	−73.57	57.19	52.89	−48.54	−54.06
	MP2/6-311+G(d,p)	31.26	66.94	−36.07	−78.38	50.09	57.95	−43.36	−60.07
PS3	MP2/6-31G*	41.65	−103.48	81.59	−73.74	105.97	−48.22	−70.71	71.41
	MP2/6-311+G(d,p)	44.99	−106.56	80.65	−72.43	106.02	−48.80	−70.80	69.71
PS4	MP2/6-31G*	123.84	−82.72	58.89	−91.62	120.48	−77.93	57.97	−89.01
	MP2/6-311+G(d,p)	122.90	−81.74	59.86	−93.75	121.21	−78.15	59.67	−91.10
PS5	MP2/6-31G*	45.11	48.66	−100.99	88.01	−94.56	54.16	55.62	−124.95
	MP2/6-311+G(d,p)	42.68	51.11	−100.98	87.31	−95.90	55.32	55.76	−123.73
PS10	MP2/6-31G*	114.42	−45.77	−41.99	108.56	−108.58	42.01	45.75	−114.39
	MP2/6−311+G(d,p)	114.71	−44.95	−42.71	109.58	−109.58	42.71	44.95	−114.70
SO1	MP2/6-31G*	105.14	−72.25	66.80	−107.52	53.74	58.85	−66.33	−42.54
	MP2/6-311+G(d,p)	104.87	−71.93	66.97	−108.21	53.47	60.26	−67.58	−42.25
	B3LYP/6-31G*	105.00	−73.11	67.28	−105.82	52.51	59.38	−65.97	−42.14
SO2	MP2/6-31G*	33.03	66.86	−34.79	−73.70	44.73	60.77	−32.32	−69.34
	MP2/6-311+G(d,p)	31.26	68.85	−34.69	−74.26	39.98	62.35	−31.90	−70.16
SO3	MP2/6-31G*	50.73	−111.82	75.87	−68.17	101.67	−42.20	−79.43	69.75
	MP2/6-311+G(d,p)	52.03	−112.86	75.90	−68.32	102.77	−43.50	−78.13	68.37
	B3LYP/6-31G*	50.01	−110.77	75.46	−67.34	101.27	−42.39	−78.28	69.80
SO4	MP2/6-31G*	117.48	−85.72	63.09	−91.57	115.73	−80.13	64.78	−89.69
	MP2/6-311+G(d,p)	118.80	−85.82	62.04	−92.10	118.19	−80.11	63.44	−88.76
SO5	MP2/6-31G*	53.75	40.02	−101.27	90.60	−92.74	54.37	54.27	−127.83
	MP2/6-311+G(d,p)	54.08	39.51	−101.33	91.48	−93.37	54.26	54.42	−128.51
SO10	MP2/6-31G*	112.27	−47.28	−44.11	108.20	−108.20	44.12	47.27	−112.26
	MP2/6-311+G(d,p)	112.46	−46.52	−44.52	109.32	−109.32	44.53	46.51	−112.46

[a] ω_i's are the dihedral angles of a ring W–X–Y–Z fragment and are placed on structure 3PS above the central bond, X–Y, of that fragment. The *i*'s increment in a clockwise fashion as you look at the ring from the face bearing the peroxide (O–O) or oxide (O) linkage.
[b] The number after the descriptor, PS or SO, refer to its relative energy at the MP2/6-31G* level.

TABLE 2 A Comparison of **3**(X = S) Persulfoxides with the Shortest Sulfur–Sulfur Distances and Their Homologous Sulfoxides

	E(kcal mol^{-1})[a]	d_{S-S}(Å)[a]		E(kcal mol^{-1})[b]	d_{S-S} (Å)[b]
3PS1	0	3.16	3SO1	0	3.29
3PS2	2.28	3.03	3SO2	4.31	3.15
3PS3	3.09	4.15	3SO3	0.28	4.23
3PS4	3.40	3.24	3SO4	1.63	3.41
3PS5	4.68	3.84	3SO5	2.06	3.83
3PS10	8.11	3.47	3SO10	4.57	3.57

[a]Relative energies and distances at the MP2/6-31G(d) computational level.
[b]Relative energies and distances at the MP2/6-311+G(d,p) computational level.

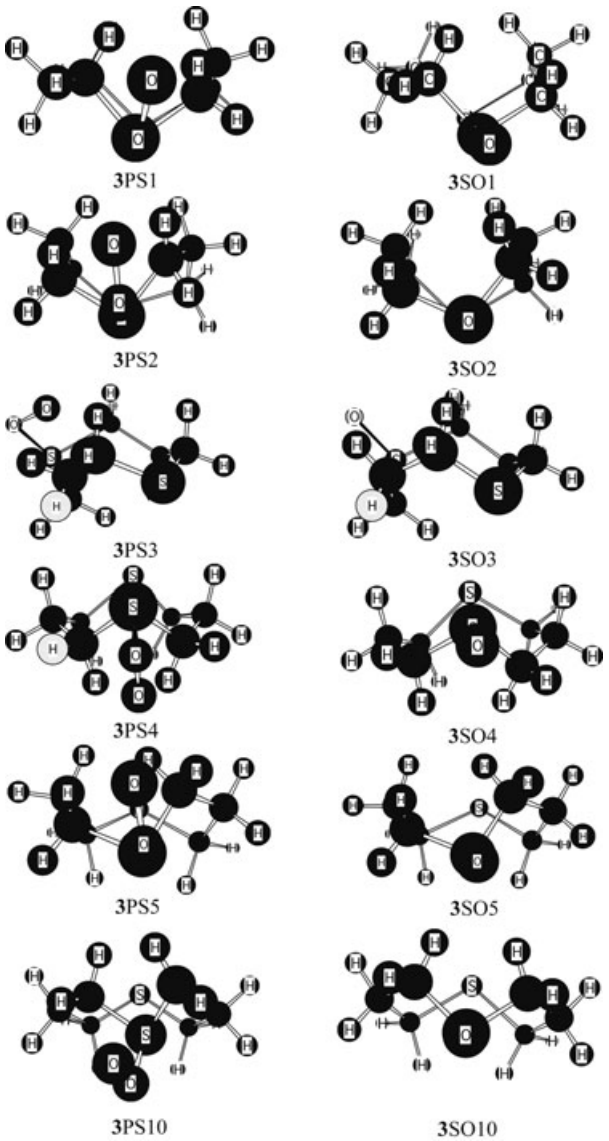

FIGURE 2 Comparison of conformational projections of MP2/6-31G(d) minimized structures of six **3**(X = S) persulfoxides and six **3SO**(X = S) sulfoxides with short intramolecular S–S distances.

remarkably similar. The most stable persulfoxide, **3PS1**, and **3PS3** adopt boat–chair conformations very similar to the global minimum in cyclooctane [20]. On the other hand, **3PS2** adopts a boat–boat conformation that does not correspond to a low-energy conformation in either cyclooctane or **3** [20]. **3PS4** is in an unusual chair–chair conformation. **3PS5** adopts a twist-boat–chair conformation that, like the boat–chair conformation, has a relatively high population in cyclooctane [20]. Finally, **3PS10** adopts a C_s symmetric twist-chair conformation with the plane of symmetry containing both sulfurs and oxygens. This plane is best observed in the projection of **3SO10** in Fig. 2.

The sulfur–sulfur distance in all the low-energy persulfoxide conformations depicted in Fig. 2, with the exception of **3PS3**, are shorter than that calculated (3.86 Å; MP2/6-31G(d)) for the sulfur–sulfur distance in the twist-boat chair global minimum in **3**(X = S). Decomposition of the persulfoxide via the physical quenching channel, k_q in Scheme 1, is significantly exothermic [9] suggesting that the close encounter between the heteroatoms in the persulfoxides is preserved in the physical quenching transition state. We suggest that this is the fundamental reason for the enhance efficiency for reaction of **3**(X = S) with singlet oxygen. Furthermore, we suggest that the stability of the persulfoxides depicted in Fig. 2 is in part because of electron donation of lone-pair electron density from the remote heteroatom into the antibonding S—O persulfoxide bond.

In order to explore the interaction between the two heteroatoms in the persulfoxides derived from **3**, we have used a natural bond order analysis (NBO) [22]. A natural bond order analysis takes the basis set and converts it into localized basis sets, NBOs, which are familiar to chemists when they deal with localized bonds visualized by Lewis dot structures. Most importantly, these NBOs can be used to calculate the magnitude of donor–acceptor interactions

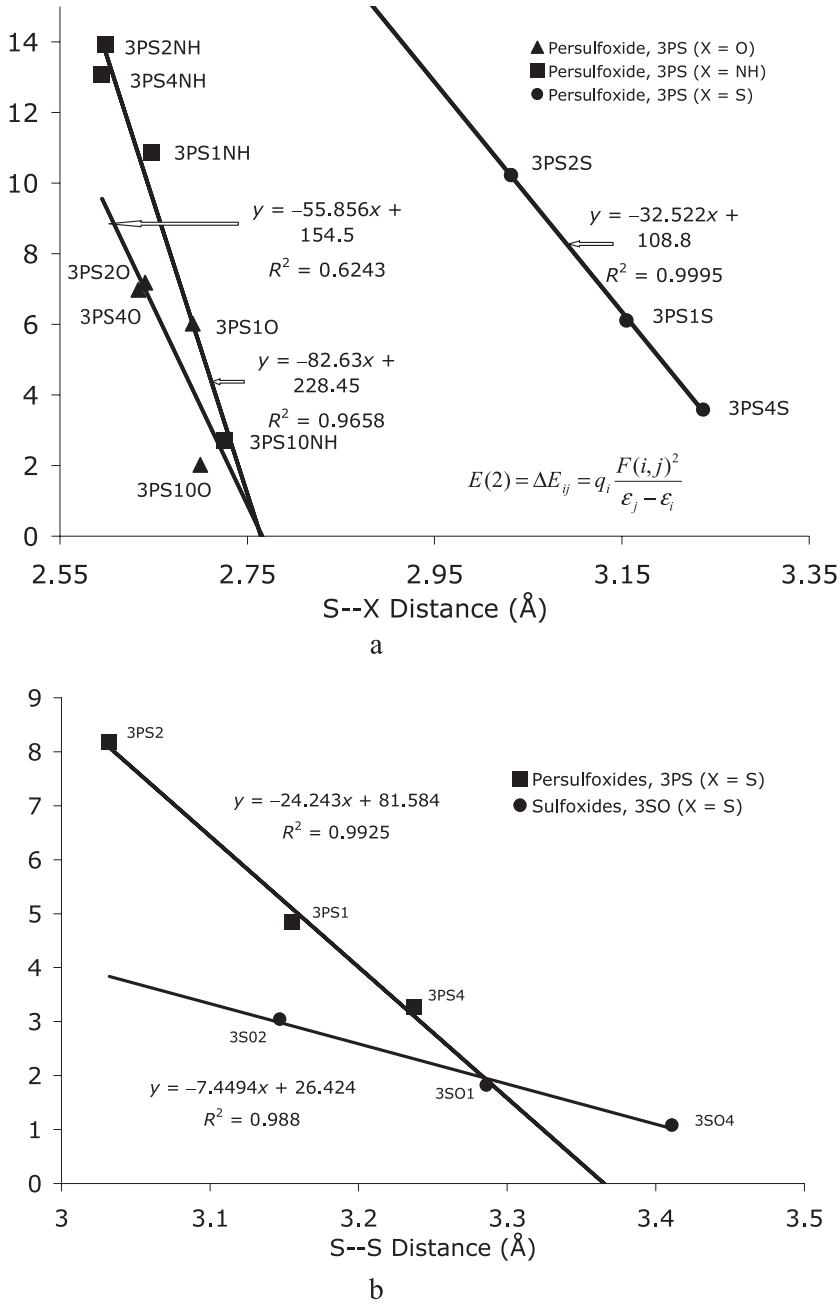

FIGURE 3 (a) Second-order perturbative interaction MP2/6-31G(d) energies as a function of S–X distance in **3PS** (X = O, NH, and S). (b) A comparison of second-order perturbative interaction MP2/6-311+G(d,p) energies for **3PS**(X = S) and **3SO** (X = S).

[23]. These donor acceptor interactions are quantitatively expressed as second-order perturbative interaction energies as expressed by the equation given in Fig. 3a. The stabilization energy, $E(2)$, associated with the donor–acceptor interaction from the ith donor to the jth acceptor NBO is a function of the donor orbital occupancy, q_i, the orbital energies, ε_i and ε_j, and the off-diagonal Fock matrix element, $F(i,j)$.

Figure 3a is a plot of these second-order perturbative energies at the MP2/6-31G(d) level for persulfoxides **3PS** (X = O), **3PS** (X = NH), and **3PS** (X = S) versus the X-persulfoxide sulfur distance. As anticipated, these interaction energies decrease as a function of the distance between the remote heteroatom and the persulfoxide sulfur. The slope of the correlation lines (i.e., the change in interaction energy per angstrom) is a direct measure of the

donorphilicity of the remote heteroatom and suggests that NH and O are both better donor atoms than sulfur. Figure 3b is a plot of the second-order perturbative energies at the MP2/6-311+G(d,p) level for persulfoxides **3PS** (X = S) and their homologous sulfoxides, **3SO** (X = S). This plot demonstrates that remote participation is more important in persulfoxides than in sulfoxides. This is consistent with a reduced positive charge at the sulfoxide sulfur in comparison to the persulfoxide sulfur as a result of π-donation from the appended oxygen.

CONCLUSION

Persulfoxide stability directly determines the overall quantum yield for the reactions of singlet oxygen with organosulfides. This study demonstrates that this stability can be dramatically influenced by nearby heteroatoms that can contribute electron density to the persulfoxide sulfur. The magnitude of this contribution depends on the ability to adopt a collinear *donor(X)-persulfoxide sulfur-oxygen* array at a *donor(X)-persulfoxide sulfur* distance less than the sum of the Van der Waals radii of X and S. This finding can potentially have important implications in directing the site of oxidation in proteins and other natural products.

EXPERIMENTAL SECTION

1,5-Dithiacylcooctane was synthesized as reported in the literature [13]. The kinetic studies were carried out using the Nd:YAG-based system described previously [24].

Kinetic Isotope Effect

The kinetic isotope effect studies were carried out by irradiation of a CD_3CN solution containing 6.25×10^{-4} M methylene blue and 0.0125 M **3d$_4$** under continuous oxygen agitation with a 150-W tungsten/halogen lamp through 1 cm of a saturated $NaNO_2$ filter solution for 10 min. The reaction mixtures were analyzed immediately by proton NMR, and the isotope effects were determined by integration of the appropriate regions.

Theoretical Studies

MP2 and DFT studies were carried out using the Gaussian 03 program package [25]. The DFT calculations used the well-established B3LYP functional [26]. The stationary points from the MP2/6-31G(d) calculations were all characterized by frequency calculations. The MP2/6-31G(d) stationary points were used as a starting point for the MP2/6-311+G(d,p) calculations.

REFERENCES

[1] Foote, C. S.; Clennan, E. L. In Active Oxygen in Chemistry; Foote, C. S.; Valentine, J. S.; Greenberg, A.; Liebman, J. F., Eds.; Blackie Academic & Professional: New York, 1995; pp. 105–140.
[2] Clennan, E. L. Tetrahedron 2000, 56, 9151–9179.
[3] Clennan, E. L. In Synthetic Organic Photochemistry; Marcel Dekker: New York, 2005; pp. 365–390.
[4] Clennan, E. L.; Pace, A. Tetrahedron 2005, 61, 6665–6691.
[5] Castano, A. P.; Mroz, P.; Hamblin, M. R. Nature Rev Cancer 2006, 6, 535–545.
[6] Qiang, Y.-g.; Zhang, X.-p.; Li, J.; Huang, Z. Chin Med J Beijing, Eng Ed 2006, 119, 845–857.
[7] Stylli, S. S.; Kaye, A. H. J. Clin Neurosci 2006, 13, 615–625.
[8] Schenck, G. O.; Krauch, C. H. Angew Chem 1962, 74, 510.
[9] Jensen, F.; Greer, A.; Clennan, E. L. J Am Chem Soc 1998, 120, 4439–4449.
[10] Clennan, E. L. Acc Chem Res 2001, 34, 875–884.
[11] Sysak, P. K.; Foote, C. S.; Ching, T.-Y. Photochem Photobiol 1977, 26, 19–27.
[12] Clennan, E. L.; Hightower, S. E.; Greer, A. J Am Chem Soc 2005, 127, 11819–11826.
[13] Clennan, E. L.; Wang, D.-X.; Yang, K.; Hodgson, D. J.; Oki, A. R. J Am Chem Soc 1992, 114, 3021–3027.
[14] Sheu, C.; Foote, C. S.; Gu, C.-L. J Am Chem Soc 1992, 114, 3015–3021.
[15] Higgins, R.; Foote, C. S.; Cheng, H. In Advances in Chemistry Series; Gould, R. F. (Ed.); American Chemical Society: Washington DC, 1968; Vol. 77, pp. 102–117.
[16] Ogilby, P. R.; Foote, C. S. J Am Chem Soc 1983, 105, 3423–3430.
[17] Liang, J.-J.; Gu, C.-L.; Kacher, M. L.; Foote, C. S. J Am Chem Soc 1983, 105, 4717–4721.
[18] Clennan, E. L.; Liao, C. Tetrahedron 2006, 62, 10724–10728.
[19] Nakayama, N.; Takahashi, O.; Kikuchi, O.; Furukawa, N. Heteroatom Chem 1999, 10, 159–166.
[20] Anet, F. A. L. In Topics in Current Chemistry; Boschke, F., Ed.; Springer-Verlag: New York, 1974; pp. 169–220.
[21] Bondi, A. J Phys Chem 1964, 68, 441–451.
[22] Reed, A. E.; Curtiss, L. A.; Weinhold, F. Chem Rev 1988, 88, 899–926.
[23] Clennan, E. L.; Hightower, S. E. J Org Chem 2006, 71, 1247–1250.
[24] Clennan, E. L.; Noe, L. J.; Wen, T.; Szneler, E. J Org Chem 1989, 54, 3581–3584.
[25] Frisch, M. J.; Trucks, G. W.; Schlegel, H. B.; Scuseria, G. E.; Robb, M. A.; Cheeseman, J. R.; Montgomery, J. A., Jr.; Vreven, T.; Kudin, K. N.; Burant, J. C.; Millam, J. M.; Iyengar, S. S.; Tomasi, J.; Barone, V.; Mennucci, B.; Cossi, M.; Scalmani, G.; Rega, N.; Petersson, G. A.; Honda, H.; Kitao, O.; Nakai,

H.; Klene, M.; Li, X.; Knox, J. E.; Hratchian, H. P.; Cross, J. B.; Adamo, C.; Jaramillo, J.; Gomperts, R.; Stratmann, R. E.; Yazyev, O.; Austin, A. J.; Cammi, R.; Pomelli, C.; Ochterski, J. W.; Ayala, P. Y.; Morokuma, K.; Voth, G. A.; Salvador, P.; Dannenberg, J. J.; Zakrzewski, V. G.; Dapprich, S.; Daniels, A. D.; Strain, M. C.; Farkas, O.; Malick, D. K.; Rabuck, A. D.; Raghavachari, K.; Foresman, J. B.; Ortiz, J. V.; Cui, Z.; Baboul, A. G.; Clifford, S.; Cioslowski, J.; Stefanov, B. B.; Liu, G.; Liashendo, A.; Piskorz, P.; Komaromi, I.; Martin, R. L.; Fox, D. J.; Keith, T.; Al-Laham, M. A.; Peng, C. Y.; Nanayakkara, A.; Challacombe, M.; Gill, P. M. W.; Johnson, B.; Chen, W.; Wong, M. W.; Gonzalez, C.; Pople, J. A. Gaussian 03, Revision A.1, Gaussian, Inc., Pittsburgh PA; 2003.

[26] (a) Becke, A. D. J Chem Phys 1993, 98, 5648–5652; (b) Lee, C.; Yang, W.; Parr, R. G. Phys Rev B 1988, 37, 785–789.